Zoologischer Anzeiger
September 2022, Volume 300 Pages 92-101
https://doi.org/10.1016/j.jcz.2022.08.001
https://archimer.ifremer.fr/doc/00788/90033/

Ryuguderes casarrubiosi sp. nov., a new deep-sea representative of the enigmatic genus *Ryuguderes* (Kinorhyncha: Cyclorhagida: Campyloderidae) from the Indian Ocean

Cepeda Diego [1, *], Sánchez Nuria [2], Olu Karine [1], Zeppilli Daniela [1]

[1] Institut Français de Recherche pour l'Exploitation de la Mer (IFREMER), Centre de Bretagne, Biologie et Ecologie des Ecosystèmes marins Profonds (BEEP), ZI de la Pointe du Diable, CS10070, 29280, Plouzané, France
[2] Universidad Complutense de Madrid (UCM), Facultad de Biología, Departamento de Biodiversidad, Ecología y Evolución (BEE), C/ José Antonio Novais 12, 28040, Madrid, Spain

* Corresponding author : Diego Cepeda, email address : dcepedag@ifremer.fr

Abstract :

A new species of the rare genus Ryuguderes is described from a deep-sea muddy seafloor part of a cold seep area at the Mozambique Channel (western Indian Ocean). The new species is easily distinguished from its only known congener by the arrangement of the middorsal (segments 2–9 in Ryuguderes iejimaensis vs. segments 1–10 in the new species) and the lateroventral acicular spines (segments 4 and 6–9 in R; iejimaensis vs. segments 3–4 and 6–9 in the new species) as well as the ventromedial female papillae (segments 6–7 in R. iejimaensis vs. segments 6–8 in the new species). Despite the ecological peculiarities of the habitat where the new species was found, all the examined specimens were recovered outside any active pockmark, which could point towards a lack of adaptation to the extreme environmental conditions associated with cold seeps.

Keywords : Kinorhynchs, Mud dragons, Cold seeps, Deep-sea, Mozambique Channel, Taxonomy.

1. Introduction

The family Campyloderidae Remane, 1929 encompasses a low diverse group of Kinorhyncha accommodating the two genera *Campyloderes* Zelinka, 1907 and the more recently established *Ryuguderes* Yamasaki, 2016 (Sørensen et al. 2015; Yamasaki 2016). Campyloderidae represents a well-supported monophyletic taxon based on a total-evidence phylogeny, but its exact position and relationships with the remaining kinorhynch clades are still far from being truly understood (Sørensen et al. 2015). In addition, the former phylogenetic analysis only included data from *Campyloderes*, so the monophyly of the clade composed of *Campyloderes* and *Ryuguderes* needs to be tested. The currently known morphological synapomorphies of the group are: (1) mouth cone with outer oral styles proximally fused (at least at their surface), (2) introvert primary spinoscalids with a minimum of eight internal septa, and (3) significantly broad midventral placid (>25 μm) and remaining ones alternatingly narrow and broad (Sørensen et al. 2015; Yamasaki 2016).

Until the description of *Ryuguderes iejimaensis* Yamasaki, 2016 from a submarine cave at the Ryukyu Archipelago (western Pacific Ocean) by Yamasaki (2016), Campyloderidae exclusively contained *Campyloderes*, with two potentially conspecific species: *Campyloderes macquariae* Johnston, 1938 and *C. vanhoeffeni* Zelinka, 1913 (Neuhaus & Sørensen 2013). Currently, both campyloderid genera are mainly distinguished by the fusion degree of the outer oral styles in their proximal part (superficially fused, still individually discernible in *Ryuguderes* vs. completely fused in *Campyloderes*), the morphology of the outer oral styles (with several filiform cuticular elements on each side of their distal part in *Ryuguderes* vs. without such elements in *Campyloderes*), the number of scalids per even-numbered sectors in rings 03–05 (0, 2 and 1 in *Ryuguderes* vs. 2, 1 and 0 in *Campyloderes*), the distribution of middorsal (absent on segment 1 in *Ryuguderes* vs. present in *Campyloderes*) and lateroventral/ventrolateral spines (absent on segments 1–3 in *Ryuguderes* vs. present in *Campyloderes*), and kind and arrangement of cuticular hairs (dense bristles of hairs through the tergosternal junctions of segments 2–9 and the middorsal line of at least segments 1–9 in *Ryuguderes* vs. without such bristles in *Campyloderes*) (Yamasaki 2016).

In the present contribution, we increase the number of representatives of the family Campyloderidae, and more specifically, of *Ryuguderes*, with the description of a new species from the deep-sea area at the Mozambique Channel (western Indian Ocean).

2. Material and methods

The studied location comprehends a deep-sea cold seep area defined by the presence of several pockmark clusters at the Mozambique Channel (western Indian Ocean), and is specifically located on the so-called Betsiboka slope, ~50 km off the Betsiboka river mouth, S 15° 21.685–21.695 E 45° 57.378–57.388, at 754–757 m depth (Fig. 1A-B). Two sediment samples in the same site were taken outside any active pockmark at different times, one during the *PAMELA–MOZ01* sampling campaign aboard the R/V *L'Atalante* in October 2014 (Olu 2014) and other during the *PAMELA–MOZ04* sampling campaign aboard the R/V *Pourquoi pas?* in November to December 2015 (Jouet & Deville 2015), both using a Barnett-type multi-corer, with three cores of 6.2 cm inner diameter.

Each core sample was horizontally divided in five, 1 cm-depth layers, and sediment of each layer was subsequently fixed in 4% buffered formalin. Sediments were passed through 1 mm and 32 µm sieves, and meiofauna was extracted using LUDOX® colloidal silica by centrifugation following the procedures of Heip et al. (1985). Specimens of the new species were subsequently picked up and prepared for light microscopy (LM) through a graded series of glycerine, and mounted on glass slides with Fluoromount G® mounting medium. Mounted specimens were photographed and studied using a Leica® DM2500 LED compound microscope equipped with differential interference contrast (DIC). Due to the low number of specimens, preparation of some of them for scanning electron microscopy was not possible. Line drawings and image plate composition were done using Adobe® Photoshop and Illustrator CC-2014 software. Type and additional material was deposited at the Natural History Museum of Denmark (NHMD).

3. Results

Taxonomic account

Class **Cyclorhagida** (Zelinka, 1896) Herranz et al., 2022

Order **Xenosomata** (Zelinka, 1907) Herranz et al., 2022

Family **Campyloderidae** Remane, 1929

Genus ***Ryuguderes*** Yamasaki, 2016

Ryuguderes casarrubiosi sp. nov.

Zoobank code: urn:lsid:zoobank.org:act:B3EC7B92–B057–4B02–8D4F–8026C85EC22B

(Figs. 2–5 and Tables 1–3)

3.1 Synonymy

Ryuguderes sp. — in Cepeda et al. 2020: p. 20, Table 2 and Fig. 12; p. 22, Fig. 13; Supplementary Material, Supplementary Fig. 2.5.

3.2 Type material

Holotype, adult female, collected in October 2014 at the Mozambique Channel in muddy sediment, western Indian Ocean (S 15° 21.685–21.695 E 45° 57.378–57.388), 754–757 m depth, deposited at NHMD under accession number NHMD-1174547. Paratypes, one adult male and one adult female, collected in October 2014 and November to December 2015, same collecting data as holotype, deposited at NHMD under accession numbers NHMD-672702 and 672705.

3.3 Non-type material

One pre-adult male and one juvenile, same collecting data as type material, deposited at NHMD under accession numbers NHMD-672703 and 672704.

3.4 Diagnosis

Acicular spines in middorsal position on segments 1–9(10) (females) and 1–11 (males), laterodorsal position on segment 10 (males), lateroventral position on segments 3–4 and 6–9 and lateral accessory position on segment 5. Short, blunt spines in lateroventral position on segment 5. Female papillae in ventromedial position on segments 6–8 (those of segment 6 more lateral but still in ventromedial position).

3.5 Etymology

The species is named after Alberto González Casarrubios, friend, colleague, and highly motivated student of the authors, who has always been fascinated with these tiny marine creatures since the very beginning of his career.

3.6 Description

Adults with retractable head, neck, and 11 trunk segments (Figs. 2A-B, 3A-B). See Table 1 for summary of spine, sensory spot, glandular cell outlet, papilla and nephridiopore locations, and Tables 2–3 for measurements and dimensions.

Head composed of mouth cone and introvert (Figs. 2D, 3D-F). None of the examined specimens had the head completely everted, but some structures could be observed inside the trunk, hence details of some structures are provided. Ring 00 of mouth cone with nine, equally sized, non-articulated outer oral styles (Figs. 2D, 3D). Outer oral styles proximally fused only at the surface (incomplete fusion), with distinct, non-fused distal parts bearing several filiform, cuticular lateral elements (Figs. 2D, 3D). Scalids with basal sheath, distally pointed end-piece and several internal septa (a minimum of eight was counted) (Fig. 3E-F). Posteriormost ring of introvert with 14 a trichoscalids superficially covered by minute hairs (Fig. 2A-B).

Neck with 14 trapezoidal placids, up to twice as long as wide, with distinct joint between the neck and the first trunk segment (Figs. 2A-B, 3G). Midventral placid significantly widest (ca. 31–42 µm wide at base), remaining ones alternating between conspicuously wider (ca. 16–23 µm wide at base) and narrower (ca. 12–15 µm wide at base) (Figs. 2A-B, 3G).

Trunk rectangular (Figs. 2A-B, 3A-B), heart-shaped in cross-section, almost constant in width but reaching the maximum sternal width at segment 8, ca. 20–24% of the total trunk length (Table 2), then progressively tapering. Segment 1 as closed, ring-like, cuticular plate; remaining segments with one tergal and two sternal plates (Figs. 2A-C, 3A-B). Pachycycli strongly sclerotized (Figs. 4A-B, E-I, 5A-I). Cuticular surface regularly covered by minute, scale-like, cuticular hairs; denser bristles of hairs through the tergosternal junctions of segments 2–9 and the middorsal line of segments 1–10 (Fig. 2A-C). Posterior segment margins straight, bearing long, flexible primary pectinate fringes (Figs. 2A-C, 4A, G-H); detailed morphology of primary pectinate fringe tips not observed. Secondary pectinate fringes as three traverse, slightly wavy rows on segments 2–10, the former two at the same level as the glandular cell outlets, the third one near the posterior segment margin, not always visible dorsally; as a single traverse, slightly wavy row on segment 11, at the same level as the glandular cell outlets (Figs. 2A-C, 4C-D, G-H, 5B).

Segment 1 with unpaired acicular spine in middorsal position (Figs. 2A, 4A-B). Three pairs of glandular cell outlets in subdorsal position, one pair in lateroventral and ventrolateral positions (Figs. 2A-B, 4A-B, E); one or two pairs of the aforementioned subdorsal glandular cell outlets near the posterior segment margin (one specimen with two pairs, two specimens with a single pair) (Figs. 2A, 4A-B). On this and following segments, glandular cell outlets are type I, with circular to oval openings (Figs. 2A-C, 4A-B; E-F, H-I, 5A-H) that may vary in shape and/or size between specimens, as well as between right and left sides of the same segment. Paired sensory spots in laterodorsal position, at the same level as the glandular cell

outlets (Figs. 2A, 4A-B). On this and following segments, sensory spots are large (except those in paradorsal position), circular to oval areas with a single, two or up to three central pores (Figs. 2A-C, 4A-I, 5A-F).

Segment 2 with unpaired acicular spine in middorsal position (Figs. 2A, 4A-B). Two pairs of glandular cell outlets in subdorsal position, and one pair in ventrolateral and ventromedial positions (Figs. 2A-B, 4A-B, E). Intraspecific variation in the position of the subdorsal glandular cell outlets was observed, as one female specimen had one pair displaced to laterodorsal position (Fig. 4B). Paired sensory spots in laterodorsal and ventromedial positions, the former at the same level as the glandular cell outlets, the latter posterior to the ventromedial glandular cell outlets longitudinally aligned with them (Figs. 2A-B, 4A-B, E).

Segment 3 with unpaired acicular spine in middorsal position, and paired in lateroventral position (Figs. 2A-B, 4A-B, F-G). Paired glandular cell outlets in subdorsal, laterodorsal, ventrolateral and ventromedial positions (Figs. 2A-B, 4A-B, E). Paired sensory spots in paradorsal and midlateral positions (Figs. 2A-B, 4A-B); on this and following segments, paradorsal sensory spots are conspicuously smaller than the remaining sensory spots, at the base of the middorsal acicular spine (Figs. 2A-C, 4C-D).

Segment 4 with unpaired acicular spine in middorsal position, and paired in lateroventral position (Figs. 2A-B, 4C, F-G). Paired glandular cell outlets in subdorsal, laterodorsal, ventrolateral and ventromedial positions (Figs. 2A-B, 4F). Unpaired sensory spot in paradorsal position at the left side of the spine, and paired in midlateral and ventromedial positions (Figs. 2A-B, 4C, F).

Segment 5 with unpaired acicular spine in middorsal position, and paired in lateral accessory position; paired blunt, small (ca. 12–15 µm length, Table 3) spines in lateroventral position (Figs. 2A-B, 4F-G). Paired glandular cell outlets in subdorsal, laterodorsal, ventrolateral and ventromedial positions (Figs. 2A-B, 4F). Paired sensory spots in paradorsal and midlateral positions (Figs. 2A-B, 4F).

Segment 6 with unpaired acicular spine in middorsal position, and paired in lateroventral position (Figs. 2A-B, 4D, G-H). Paired glandular cell outlets in subdorsal, laterodorsal, ventrolateral and ventromedial positions (Figs. 2A-B, 4H-I, 5F). Paired sensory spots in paradorsal, midlateral and ventromedial positions (Figs. 2A-B, 4H-I, 5F). Females with paired papillae in ventromedial position (Figs. 2B, 4H-I).

Segment 7 similar to segment 6 in the arrangement of spines, glandular cell outlets and sensory spots; females with paired papillae in ventromedial position but more mesial than those of preceding segment (Figs. 2A-B, 4H, 5F).

Segment 8 similar to segment 7 in the arrangement of spines, glandular cell outlets, sensory spots and female papillae, but with an extra pair of ventromedial glandular cell outlets at the same level as the other ventromedial pair (Figs. 2A-B, 5A-C).

Segment 9 with unpaired acicular spine in middorsal position, and paired in lateroventral position (Figs. 2A-C, 5C-D, G). Two pairs of glandular cell outlets in ventromedial position (one of them near the posterior segment margin), and one pair in subdorsal, laterodorsal and ventrolateral positions (Fig. 2A-B). Unpaired sensory spot in paradorsal position at the right side of the spine, and paired in midlateral, lateroventral and ventromedial positions (Figs. 2A-B, 5C). Nephridiopores in lateral accessory position as small, oval sieve plates (Figs. 2B, 5C).

Segment 10 with unpaired acicular spine in middorsal position in both sexes, and paired in laterodorsal position only in males (Figs. 2A, C, 5D, G). The female paratype (NHMD-672705) had the middorsal bristle of hairs and the base of the acicular spine, but the spine itself is missing. Two to three pairs of glandular cell outlets in subdorsal position, and one pair in ventrolateral and ventromedial positions (Figs. 2A-C, 5D-E, G-H). One pair of sensory spots in subdorsal position, and two pairs in midlateral position closely located each other, and one pair in ventromedial position (Figs. 2A-C, 5C-E, G-H).

Segment 11 with unpaired acicular spine in middorsal position only in males, without the basal bristle of hairs (Figs. 2C, 5G). Paired glandular cell outlets in subdorsal, ventrolateral and ventromedial positions (Figs. 2A-C, 5D-E, G-H). Paired sensory spots in subdorsal and ventromedial positions (Figs. 2A-C, 5D-E). Unpaired midterminal and paired lateral terminal and lateral terminal accessory acicular spines with thick proximal cuticle around central longitudinal cavity; midterminal and lateral terminal accessory spines with conspicuous pores connected to subcuticular cavity through ducts (Figs. 2A-C, 3A-B, 5D-E, G-I). Midterminal and lateral terminal accessory spines variable in length compared to total trunk length (MTS:TL ratio of ca. 18–42%, LTAS:TL ratio of ca. 34–87%, Table 2), the latter up to twice as longer as the former (MTS:LTAS ratio of ca. 45–52%, Table 2); lateral terminal spines conspicuously short (LTS:TL ratio of ca. 8–14%, LTS:LTAS ratio of ca. 13–29%, Table 2). Wide, oval gonopores in ventrolateral position only in females, near the anterior segment margin (Figs. 2B,

5I). Posterior edges of tergal plate trapezoidal, distally pointed (Figs. 2A-C, 5D-E). Posterior edge of sternal plates short, wide, distally rounded (Fig. 2B).

3.7 Remarks on juvenile and pre-adult stages

A single juvenile specimen, likely a juvenile stage 2, was examined (Fig. 3C). The characteristic outer oral styles of the genus, with incompletely fused basal regions and non-fused distal parts bearing lateral filiform, cuticular elements are visible. The trunk is more cigar-shaped, composed of 10 segments, with quite inconspicuous separation between segments 9 and 10 (Fig. 3C, I). Segment 9 longest (ca. 40.2 µm length), remaining ones ranging ca. 17.7–25.0 µm length. Pachycycli, secondary pectinate fringes, tergosternal and midventral junctions, gonads, glandular cell outlets, lateral terminal spines, sensory spots, papillae and hairs absent or scarcely developed, cuticle much thinner and softer than that of adults (Fig. 3C, I). Several light-refracting vesicles inside trunk segments (Fig. 3I). Middorsal spines present throughout segments 1–10, lateroventral spines throughout segments 3–9; midterminal and lateral terminal accessory spines on segment 10 (Fig. 3I). Spines conspicuously longer than those of the adults; middorsal spine of segment 9, midterminal spine and lateral terminal accessory spines with spherical, enlarged bases; midterminal spine longer than lateral terminal accessory spines (Fig. 3I). Posterior edges of tergal plate of segment 11 small, distally rounded (Fig. 3I).

A single pre-adult, male specimen was also studied (Fig. 3H). The most remarkable difference with the adults was the thinner, softer cuticle, and the less conspicuous cuticular appendages and secondary pectinate fringes (Fig. 3H). The specimen already had the gonads completely developed as well as the middorsal and laterodorsal, male sexually dimorphic spines on segment 10 (Fig. 3H).

3.8 Kinorhynch associated fauna

The new species co-occurred in the studied area with *Condyloderes* sp., *Echinoderes apex* Yamasaki et al., 2018a, *E.* cf. *dubiosus*, *E. unispinosus* Yamasaki et al., 2018b and *Fujuriphyes hydra* Cepeda et al., 2020.

4. Discussion

4.1 Remarks on taxonomic features

Morphological cuticular structures of the new species described herein entail assigning it to the family Campyloderidae. The presence of proximally fused outer oral styles, primary spinoscalids internally divided by a minimum of eight septa, number, shape and arrangement of placids (14 placids, the midventral one widest and the remaining ones alternating between wider and narrower) as well as the distribution of acicular and blunt spines (acicular spines located middorsally on segments 1–11 in males and 1–10 in females; lateroventrally on segments 3–4 and 6–9; in lateral accessory position on segment 5; and lateroventral, blunt, short spines on segment 5) generally follows the diagnostic pattern described for campyloderids (Sørensen et al. 2015; Yamasaki 2016). In addition, the mouth cone of *Ryuguderes casarrubiosi* sp. nov. is characterized by filiform, lateral cuticular structures at the distal part of each outer oral style. Moreover, the new species shows dense cuticular bristles of hairs on the tergosternal junctions on segments 2–9 and the middorsal line on some segments from 1–10. These two cuticular features distinguish it from species of *Campyloderes*, assigning the new species to the sister genus *Ryuguderes* (Yamasaki 2016). It must be noticed, however, the presence of regular-shaped primary pectinate fringes in *R. casarrubiosi* sp. nov., which is more similar to the morphology of these structures in *Campyloderes*, but as long as this character is not considered diagnostic in any campyloderid genus, we consider the new species to fit better within *Ryuguderes*.

To date, *Ryuguderes* was a monospecific genus with *R. iejimaensis* as its single representative (Yamasaki 2016). Both *R. casarrubiosi* sp. nov. and *R. iejimaensis* resemble each other in terms of general distribution of acicular spines, glandular cell outlets and sensory spots, but essential differences also exist. The most noticeable cuticular structure to discriminate *R. casarrubiosi* sp. nov. from its congener is the presence of middorsal spines on segments 1 and 10 in both sexes, whereas *R. iejimaensis* lacks spine on segment 1 and only males possess it on segment 10 (Yamasaki 2016). However, it must be noticed that only one of the two examined females of *R. casarrubiosi* sp. nov. possessed this spine on segment 10, whereas the other one only had the basal bristle of hairs with the actual spine missing. This could mean that females of the new species actually have a middorsal spine of segment 10 but the most distal part of the structure detached in one of the specimens. However, other two possibilities must be mentioned. Campyloderid females lack middorsal spine on segment 10, which could mean that the observed female of *R. casarrubiosi* sp. nov. bears this structure as a morphological abnormality. In addition, we could be facing another case of presence of several adult stages like in other

Kentrorhagata taxa, one female stage with middorsal spine on segment 10 and another one lacking this structure.

Likewise, the new species bears lateroventral spines on segment 3, which are absent in *R. iejimaensis* (Yamasaki 2016). The differences related to the sensory spots concern mainly the lateral and ventral series, since *R. iejimaensis* has midlateral sensory spots only on segments 3, 4, 6 and 8 (Yamasaki 2016), unlike the pattern described in *R. casarrubiosi* sp. nov., with midlateral sensory spots on segments 3–10. Moreover, the new species shows lateroventral sensory spots on segment 9 and ventromedial on segments 7 and 11, all three pairs absent in *R. iejimaensis* (Yamasaki 2016). Regarding glandular cell outlets, both species have the same number of dorsal and ventral glandular cell outlets, despite some minor difference in positions on segments 1, 2, 10 and 11 can be observed (*R. casarrubiosi* sp. nov. has on segment 1 three pairs in subdorsal position, plus one pair in lateroventral and ventrolateral positions; segment 2 with two subdorsal pairs, segment 10 with one ventrolateral and ventromedial pairs, and segment 11 with one ventrolateral and ventromedial pairs; *R. iejimaensis* has on segment 1 two pairs in laterodorsal position, plus one pair in subdorsal, ventrolateral and ventromedial positions, segment 2 with one subdorsal and one laterodorsal pairs, segment 10 with two ventrolateral pairs, segment 11 with one ventrolateral and two ventromedial pairs) (Yamasaki 2016).

Finally, both congeners also differ by the distribution of female papillae: these structures are present in ventromedial position on segments 6 and 7 in *R. iejimaensis* (Yamasaki 2016), while the new species has papillae also on segment 8.

4.2 Remarks on systematic features

Although *Campyloderes* and *Ryuguderes* share some morphological features as sister genera of Campyloderidae, other characters may be used to distinguish them. After the description of *R. iejimaensis*, these differences were: (1) fusion degree of the outer oral styles, (2) scalid arrangement per introvert sector, (3) spine arrangement throughout trunk segments, and (4) presence of dense bristles of cuticular hairs in the middorsal line and the tergosternal junctions (Yamasaki 2016). With the description of *R. casarrubiosi* sp. nov., differences in the acicular spine arrangement are less strict but still present.

306 *Ryuguderes iejimaensis* manly differed from *Campyloderes* in the absence of middorsal
307 spine on segment 1 and lateroventral spines on segments 1–3, structures otherwise present in
308 the latter (Neuhaus & Sørensen 2013; Yamasaki 2016). However, *R. casarrubiosi* sp. nov. also
309 possesses a middorsal spine on segment 1 and lateroventral spines on segment 3. Thus, the only
310 difference that should be considered regarding the spine arrangement between *Ryuguderes* and
311 *Campyloderes* is the presence of these structures throughout the lateral series of segments 1–2.

312 This fact supports the hypothesis of Yamasaki (2016) that suggests a closer phylogenetic
313 relationship between Xenosomata and Kentrorhagata. Apart from the morphological
314 similarities found by Yamasaki (2016) between *R. iejimaensis*, *Campyloderes* and some genera
315 of Kentrorhagata, including *Centroderes* Zelinka, 1907 and *Wollunquaderes* Sørensen &
316 Thormar, 2010, the presence of a middorsal acicular spine on segment 1 in *R. casarrubiosi* sp.
317 nov. furthermore agrees with the closer relationship Xenosomata-Kentrorhagata, as the
318 aforementioned kentrorhagids also possess this structure (Sørensen & Thormar 2010; Neuhaus
319 et al. 2013, 2014; Sørensen et al. 2016). In addition to this, *Campyloderes* and *Wollunquaderes*
320 also have lateroventral spines on segment 3 (Sørensen & Thormar 2010; Neuhaus & Sørensen
321 2013) as *R. casarrubiosi* sp. nov., which also supports the aforementioned hypothesis.

322 If we consider these characters (middorsal spine on segment 1 and lateral spine on
323 segment 3, plus the other features shared by Xenosomata-Kentrorhagata) as plesiomorphic for
324 the Xenosomata-Kentrorhagata group (Yamasaki 2016), the loss of the aforementioned spines
325 in *R. iejimaensis* could be interpreted as a reversion of the character state as an autapomorphy
326 of the species. Nevertheless, this hypothesis cannot be confirmed until more phylogenetic data
327 is available for the entire Xenosomata-Kentrorhagata group. *Ryuguderes* seems to play a key
328 role for understanding the morphological evolution in the Xenosomata-Kentrorhagata group, as
329 also suggested by Yamasaki (2016).

330

331 *4.3 Remarks on habitat features*

332 *Ryuguderes casarrubiosi* sp. nov. has been found in a very particular deep-sea environment
333 characterized by the presence of cold seeps, extreme habitats with a recurrent emission of
334 hydrogen sulphide, methane and other hydrocarbon-rich fluids (Torres & Bohrmann 2014).
335 Cold seeps usually induce the creation of circular to ellipsoid, shallow depressions on the
336 seafloor called pockmarks (Hovland & Judd 1988). The fauna in these habitats must not only
337 be adapted to deep-sea features but also to the particular extreme conditions of these cold

emissions, which includes high concentrations of reduced chemical substances, low oxygen level and high primary production due to chemoautotrophic microorganisms (Sibuet & Olu 1998; Levin 2005; Zeppilli et al. 2018).

Unidentified species of Kinorhyncha were found in cold seeps at the Gulf of Mexico, Mozambique Channel, Caribbean Sea, Black Sea, Mediterranean Sea and eastern Pacific Ocean off Oregon (Olu et al. 1997; Revkov & Sergeeva 2004; Robinson et al. 2004; Sommer et al. 2007; Bright et al. 2010; Zeppilli et al. 2011, 2012; Lampadariou et al. 2013; Sánchez et al. 2021). More recently, Adrianov & Maiorova (2022) have studied a methane cold seep area in the Bering Sea, revealing the presence of *Condyloderes shirleyi* Neuhaus & Higgins, 2019 in Neuhaus et al., 2019 and *Pycnophyes schornikovi* Adrianov, 1999 in Adrianov & Malakhov, 1999. Thus, knowledge on the kinorhynch fauna from cold seeps is still scarce, and only some localities with this kind of habitat have been explored to the species level.

Cepeda et al. (2020) discovered a relatively rich kinorhynch community from the studied area in the present paper (Mozambique Channel), including the presence of *Condyloderes* sp., *Echinoderes apex*, *E.* cf. *dubiosus*, *E. hviidarum* Sørensen et al., 2018, *E. unispinosus*, *Echinoderes* sp., *Fissuroderes cthulhu* Cepeda et al., 2020, *Fujuriphyes dagon* Cepeda et al., 2020, *F. hydra*, *Sphenoderes* cf. *indicus*, and the herein described *R. casarrubiosi* sp. nov. (reported as *Ryuguderes* sp. in Cepeda et al. 2020). However, of all these species, only *Condyloderes* sp., *E. hviidarum*, *E. unispinosus*, *Fi. cthulhu*, *Fu. dagon* and *S.* cf. *indicus* were recovered at actual active pockmarks (Cepeda et al. 2020). The remaining species, including *R. casarrubiosi* sp. nov., were found exclusively in the area surrounding the pockmarks. This area may receive some of the extreme environmental conditions of the active pockmarks up to some extent, but surely on a much smaller scale. The absence of *R. casarrubiosi* sp. nov. in the active pockmarks may suggest a lack of adaptation to cope with the reduced conditions of this environment.

Cold seeps seem to somehow harbour rich communities of meiofauna in which the considered "rare" meiofaunal taxa (abundance typically less than 1%) found a space to maintain stable populations (Zeppilli et al. 2018; Cepeda et al. 2020; Sánchez et al. 2021). There is still a need to promote new studies in unexplored cold seep areas worldwide to expand our knowledge of this particular habitat and, specifically, the Kinorhyncha communities that live there.

Declaration of competing interest

The authors declare that they have not known competing financial interests or personal relationships that could have appeared to influence the work reported in this paper.

Acknowledgements

This study was done within the framework of the PAssive Margin Exploration LAboratories (PAMELA) project, funded by TOTAL and IFREMER. The authors would like to express their gratitude to all the participants and staff of the R/V *L'Atalante* and *Pourquoi pas?*, Vessel, Scampi team and all scientists and students that joined the PAMELA MOZ01 and MOZ04 cruises. Moreover, the authors also thank the Ghent meiofauna laboratory for the samples processing and Dr Julie Tourolle (IFREMER) for providing the figure map.

References

Adrianov, A.V., Maiorova, A.S., 2022. Kinorhynchs (Kinorhyncha) from methane cold seeps in the Bering Sea, with biogeographical discussion and ecological notes. Deep Sea Res. II Top. Stu. Oceanogr., 105132. https://doi.org/10.1016/j.dsr2.2022.105132.

Adrianov, A.V., Malakhov, V.V., 1999. Cephalorhyncha of the World Ocean, first ed. KMK Scientific Press, Moscow.

Bright, M., Plum, C., Riavitz, L.A., Nikolov, N., Martínez-Arbizu, P., et al., 2010. Epizooic metazoan meiobenthos associated with tubeworm and mussel aggregations from cold seeps of the northern Gulf of Mexico. Deep Sea Res. II Top. Stud. Oceanogr. 57, 1982–1989. https://doi.org/10.1016/j.dsr2.2010.05.003.

Cepeda, D., Pardos, F., Zeppilli, D., Sánchez, N., 2020. Dragons of the deep sea: Kinorhyncha communities in a pockmark field at Mozambique Channel, with the description of three new species. Front. Mar. Sci. 7, 665. https://doi.org/10.3389/fmars.2020.00665.

Heip, C.H.R., Vincx, M., Vranken, G., 1985. The ecology of marine nematodes. Oceanogr. Mar. Biol. 23, 399–489.

Herranz, M., Stiller, J., Worsaae, K., Sørensen, M.V., 2022. Phylogenomic analyses of mud dragons (Kinorhyncha). Mol. Phylogenet. Evol. 168, 107375. https://doi.org/10.1016/j.ympev.2021.107375.

Hovland, M., Judd, A.G., 1988. Seabed Pockmarks and Seepages: Impact on Geology, Biology and Marine Environment, first ed. Grahamand Trotman, London.

Johnston, T.H., 1938. Report on the Echinoderida. Sci. Rep. Ser. C Zool. Bot. 10, 1–13.

Jouet, G., Deville, E., 2015. PAMELA-MOZ04 cruise, R/V *Pourquoi pas?* https://doi.org/10.17600/15000700.

Lampadariou, N., Kalogeropoulou, V., Sevastou, K., Keklikoglou, K., Sarrazin, J., 2013. Influence of chemosynthetic ecosystems on nematode community structure and biomass in the deep eastern Mediterranean Sea. Biogeosciences 10, 5381–5398. https://doi.org/10.5194/bg-10-5381-2013.

Levin, L.A., 2005. Ecology of cold seep sediments: interactions of fauna with flow, chemistry and microbes. In: Gibson, R.N., Atkinson, R.J.A., Gordon, J.D.M. (Eds.), Oceanography and Marine Biology. CRC Press, Boca Raton, U.S.A., pp. 1–46.

Neuhaus, B., Dal Zotto, M., Yamasaki, H., Higgins, R.P., 2019. Revision of *Condyloderes* (Kinorhyncha, Cyclorhagida) including description of *Condyloderes shirleyi* sp. nov. Zootaxa 4561, 1–91. https://doi.org/10.11646/zootaxa.4561.1.1.

Neuhaus, B., Pardos, F., Sørensen, M.V., Higgins, R.P., 2013. Redescription, morphology, and biogeography of *Centroderes spinosus* (Reinhard, 1881) (Kinorhyncha, Cyclorhagida) from Europe. Cah. Biol. Mar. 54, 109–131. https://doi.org/10.21411/CBM.A.8E3FD0CA.

Neuhaus, B., Pardos, F., Sørensen, M.V., Higgins, R.P., 2014. New species of *Centroderes* (Kinorhyncha: Cyclorhagida) from the Northwest Atlantic Ocean, life cycle, and ground pattern of the genus. Zootaxa 3901, 1–69. https://doi.org/10.11646/zootaxa.3901.1.1.

Neuhaus, B., Sørensen, M.V., 2013. Populations of *Campyloderes* sp. (Kinorhyncha, Cyclorhagida): one global species with significant morphological variation? Zool. Anz. 252, 48–75. https://doi.org/10.1016/j.jcz.2012.03.002.

Olu, K., 2014. PAMELA-MOZ01 cruise, R/V *L'Atalante*. https://doi.org/10.17600/14001000.

Olu, K., Lance, S., Sibuet, M., Henry, P., Fiala-Médioni, A., Dinet, A., 1997. Cold seep communities as indicators of fluid expulsion patterns through mud volcanoes seaward of the Barbados accretionary prism. Deep Sea Res. I Oceanogr. Res. Pap. 44, 811–841. https://doi.org/10.1016/S0967-0637(96)00123-9.

Remane, A., 1929. Dritte Klasse des Cladus Nemathelminthes. Kinorhyncha = Echinodera, first ed. De Gruyter, Berlin.

Revkov, N.K., Sergeeva, N.G., 2004. Current state of the zoobenthos at the Crimean shores of the Black Sea. In: Öztürk, B., Mokievsky, V.O., Topaloğlu, B. (Eds.), International Workshop on Black Sea Benthos. Turkish Marine Research Foundation TÜDAV, Istanbul, Turkey, pp 186–214.

Robinson, C.A., Bernhard, J.M., Levin, L.A., Mendoza, G.F., Blanks, J.K., 2004. Surficial hydrocarbon seep infauna from the Blake ridge (Atlantic Ocean, 2150 m) and the Gulf of Mexico (690–2240 m). Mar. Ecol. 25, 313–336. https://doi.org/10.1111/j.1439-0485.2004.00034.x.

Sánchez, N., Zeppilli, D., Baldrighi, E., Vanreusel, A., Gasimandova-Lahitsiresy, M., et al., 2021. A threefold perspective on the role of a pockmark in benthic faunal communities and biodiversity patterns. Deep Sea Res. I Oceanogr. Res. Pap. 167, 103425. https://doi.org/10.1016/j.dsr.2020.103425.

Sibuet, M., Olu, K., 1998. Biogeography, biodiversity and fluid dependence of deep-sea cold-seep communities at active and passive margins. Deep Sea Res. II Top. Stud. Oceanogr. 45, 517–567. https://doi.org/10.1016/S0967-0645(97)00074-X.

Sommer, S., Gutzmann, E., Pfannkuche, O., 2007. Sediments hosting gas hydrates: oases for metazoan meiofauna. Mar. Ecol. Prog. Ser. 337, 27–37. https://doi.org/10.3354/meps337027.

Sørensen, M.V., Dal Zotto, M., Rho, H.S., Herranz, M., Sánchez, N., et al., 2015. Phylogeny of Kinorhyncha based on morphology and two molecular loci. PLoS ONE 10, e0133440. https://doi.org/10.1371/journal.pone.0133440.

Sørensen, M.V., Gąsiorowski, L., Randsø, P.V., Sánchez, N., Neves, R.C., 2016. First report of kinorhynchs from Singapore, with the description of three new species. Raff. Bull. Zool. 64, 3–27. http://doi.org/10.5281/zenodo.4502533.

Sørensen, M.V., Thormar, J., 2010. *Wollunquaderes majkenae* gen. et sp. nov. - a new cyclorhagid kinorhynch genus and species from the Coral Sea, Australia. Mar. Biodivers. 40, 261–275. https://doi.org/10.1007/s12526-010-0048-x.

Torres, M.E., Bohrmann, G., 2014. Cold seeps. Encyclopedia of Marine Geosciences. Springer Science+Business Media, Dordrecht. https://doi.org/10.1007/978-94-007-6644-0_153-1.

Yamasaki, H., 2016. *Ryuguderes iejimaensis*, a new genus and species of Campyloderidae (Xenosomata: Cyclorhagida: Kinorhyncha) from a submarine cave in the Ryukyu Islands, Japan. Zool. Anz. 265, 69–79. https://doi.org/10.1016/j.jcz.2016.02.003.

Yamasaki, H., Neuhaus, B., George, K.H., 2018a. Three new species of Echinoderidae (Kinorhyncha: Cyclorhagida) from two seamounts and the adjacent deep-sea floor in the Northeast Atlantic Ocean. Cah. Biol. Mar. 59, 79–106. https://doi.org/10.21411/CBM.A.124081A9.

Yamasaki, H., Neuhaus, B., George, K.H., 2018b. New species of *Echinoderes* (Kinorhyncha: Cyclorhagida) from Mediterranean seamounts and from the deep-sea floor in the Northeast Atlantic Ocean, including notes on two undescribed species. Zootaxa 4387, 541–566. https://doi.org/10.11646/zootaxa.4387.3.8.

Zelinka, C., 1896. Demonstration der Tafeln der *Echinoderes* - Monographie. Verh. Dtsch. Zool. Ges. 6, 197–199.

Zelinka, C., 1907. Zur Kenntnis der Echinoderen. Zool. Anz. 32, 130–136.

Zelinka, C., 1913. Die Echinoderen der Deutschen Südpolar-Expedition 1901-1903. Deutsche Südpolar Expedition Zool. 6, 419–437.

Zeppilli, D., Canals, M., Danovaro, R., 2012. Pockmarks enhance deep-sea benthic biodiversity: a case study in the western Mediterranean Sea. Div. Distrib. 18, 832–846. https://doi.org/10.1111/j.1472-4642.2011.00859.x.

Zeppilli, D., Leduc, D., Fontanier, C., Fontaneto, D., Fuchs, S., et al., 2018. Characteristics of meiofauna in extreme marine ecosystems: a review. Mar. Biodivers. 48, 35–71. https://doi.org/10.1007/s12526-017-0815-z.

Zeppilli, D., Mea, M., Corinaldesi, C., Danovaro, R., 2011. Mud volcanoes in the Mediterranean Sea are hot spots of exclusive meiobenthic species. Prog. Oceanogr. 91, 260–272. https://doi.org/10.1016/j.pocean.2011.01.001.

TABLES.

Table 1. Summary of arrangement of spines, tubes, sensory spots, glandular cell outlets, nephridiopores and additional cuticular structures in adults of *Ryuguderes casarrubiosi* sp. nov. Abbreviations: ac, acicular spine; b, blunt spine; gco, glandular cell outlet; go, gonopore; LA, lateral accessory; LD, laterodorsal; ltas, lateral terminal accessory spine; lts, lateral terminal spine; LV, lateroventral; MD, middorsal; ML, midlateral; mts, midterminal spine; ne, nephridiopore; pa, papilla; PD, paradorsal; SD, subdorsal; ss, sensory spot; VL, ventrolateral; VM, ventromedial; ♂/♀ indicates sexually dimorphic structures; *, indicates unpaired structure; ▲, indicates structures with intraspecific variability (not present in all the examined specimens).

Segment	MD	PD	SD	LD	ML	LA	LV	VL	VM
1	ac		gco, gco, gco	ss			gco	gco	
2	ac		gco, gco	ss				gco	gco, ss
3	ac	ss	gco	gco	ss		ac	gco	gco
4	ac	ss*	gco	gco	ss		ac	gco	gco, ss
5	ac	ss	gco	gco	ss	ac	b	gco	gco
6	ac	ss	gco	gco	ss		ac	gco	pa(♀), gco, ss
7	ac	ss	gco	gco	ss		ac	gco	gco, ss, pa(♀)
8	ac	ss	gco	gco	ss		ac	gco	gco, gco, ss, pa(♀)
9	ac	ss*	gco	gco	ss	ne	ac, ss	gco	gco, gco, ss
10	ac▲		gco, gco, gco▲, ss	ac(♂)	ss, ss			gco	gco, ss
11	ac(♂), mts		gco, ss			ltas	lts	go(♀), gco	gco, ss

Table 2. Measurements of body size, lateral terminal, lateral terminal accessory and midterminal spines of type material of *Ryuguderes casarrubiosi* sp. nov. Abbreviations: LTAS, lateral terminal accessory spine; LTS, lateral terminal spine; MSW, maximum sternal width (measured at segment X); MTS, midterminal spine; S, segment length (number after S indicates corresponding segment); SW; standard sternal width (measured at segment 10); TL, total length of trunk.

Character	Holotype (♀ NHMD-1174547)	Paratype (♀ NHMD-672705)	Paratype (♂ NHMD-672702)
TL (µm)	534.9	531.2	548.6
MSW8 (µm)	126.9	105.3	121.5
MSW8/TL (%)	23.7	19.8	22.1
SW10 (µm)	116.4	96.4	109.2
SW10/TL (%)	21.8	18.1	19.9
S1 (µm)	52.9	43.8	63.0
S2 (µm)	42.1	37.8	43.6
S3 (µm)	39.2	40.7	56.4

S4 (µm)	39.5	48.1	44.6
S5 (µm)	41.7	51.9	48.7
S6 (µm)	55.3	55.8	50.3
S7 (µm)	64.2	60.9	61.6
S8 (µm)	70.7	62.4	63.5
S9 (µm)	70.8	73.1	69.9
S10 (µm)	63.5	54.7	60.2
S11 (µm)	68.8	59.2	79.1
LTS (µm)	44.0	52.0	76.8
LTS/TL (%)	8.2	9.8	14.0
LTAS (µm)	328.9	179.6	475.6
LTAS/TL (%)	61.5	33.8	86.7
LTS/LTAS (%)	13.4	28.9	16.1
MTS (µm)	147.0	94.2	229.3
MTS/TL (%)	27.5	17.7	41.8

Table 3. Measurements of middorsal, laterodorsal, lateral accessory and lateroventral spines of type material of *Ryuguderes casarrubiosi* sp. nov.. Abbreviations: ac, acicular spine; b, blunt spine; LA, lateral accessory; LD, laterodorsal; LV, lateroventral; MD, middorsal; ♂, male condition of sexually dimorphic character; number after abbreviation indicates corresponding segment.

Character	Holotype (♀ NHMD-1174547)	Paratype (♀ NHMD-672705)	Paratype (♂ NHMD-672702)
MD1 (ac) (µm)	53.8	26.3	28.5
MD2 (ac) (µm)	53.5	34.2	35.0
MD3 (ac) (µm)	54.2	33.2	32.5
MD4 (ac) (µm)	60.5	44.7	51.7
MD5 (ac) (µm)	61.9	48.5	62.4
MD6 (ac) (µm)	68.1	54.6	64.9
MD7 (ac) (µm)	64.9	61.0	59.0
MD8 (ac) (µm)	73.7	71.5	72.6
MD9 (ac) (µm)	70.5	85.1	82.6
MD10 (ac) (µm)	47.4	-	80.5
MD11 (ac, ♂) (µm)	-	-	52.0
LD10 (ac, ♂) (µm)	-	-	80.0
LV3 (ac) (µm)	46.0	24.6	44.7
LV4 (ac) (µm)	53.9	30.1	61.6

LA5 (ac) (μm)	57.9	41.5	69.1
LV5 (b) (μm)	14.5	11.7	14.5
LV6 (ac) (μm)	58.9	46.4	70.4
LV7 (ac) (μm)	64.3	46.1	73.8
LV8 (ac) (μm)	61.7	55.3	74.8
LV9 (ac) (μm)	71.8	69.3	91.5

526 **FIGURE CAPTIONS.**

527 Figure 1. Map with location of the sampling region (marked with a black star) offshore north-
528 western Madagascar margin at the Mozambique Channel with detail of the studied area (marked
529 with a red square) (A), and detailed bathymetry of the area where the new species was found
530 (red triangle). Map courtesy of Dr Julie Tourolle, created with Globe©, IFREMER.

531 Figure 2. Line art drawing of *Ryuguderes casarrubiosi* sp. nov. based on type material. A:
532 Dorsal female trunk overview; B: ventral female trunk overview; C: dorsal view of male
533 segments 10–11; D: mouth cone external ring of outer oral styles. Abbreviations: dis, distal part
534 (of outer oral style); dpl, dorsal placid; go, gonopore; lane, lateral accessory nephridiopore; las,
535 lateral accessory spine; ldgco, laterodorsal glandular cell outlet; lds, laterodorsal spine; ldss,
536 laterodorsal sensory spot; ltas, lateral terminal accessory spine; lts, lateral terminal spine; lvb,
537 lateroventral blunt spine; lvgco, lateroventral glandular cell outlet; lvs, lateroventral spine; lvss,
538 lateroventral sensory spot; mds, middorsal spine; mlss, midlateral sensory spot; mts,
539 midterminal spine; mvpl, midventral placid; oos, outer oral style; po, pore; ppdss, paired
540 paradorsal sensory spot; ppf, primary pectinate fringe; pro, proximal part (of outer oral style);
541 S, segment (followed by number of corresponding segment); sdgco, subdorsal glandular cell
542 outlet; sdss, subdorsal sensory spot; spf, secondary pectinate fringe; ts, trichoscalid; tsp,
543 trichoscalid plate; updss, unpaired paradorsal sensory spot; vlgco, ventrolateral glandular cell
544 outlet; vmgco, ventromedial glandular cell outlet; vmpa, ventromedial papilla; vmss,
545 ventromedial sensory spot.

546 Figure 3. Light micrographs of female adult holotype NHMD-1174547 (A), female adult
547 paratype NHMD-672705 (E–G), male adult paratype NHMD-672702 (B, D), male pre-adult
548 specimen NHMD-672704 (H), and J-2 juvenile specimen NHMD-67203 (C, I) of *Ryuguderes*
549 *casarrubiosi* sp. nov., showing trunk cuticular overviews and details on head, neck and
550 posterior trunk segments. A: Ventral trunk overview; B: Dorsal trunk overview; C: Ventral
551 trunk overview; D: Outer oral styles; E: detail of the scalid internal septa (indicated with
552 arrows); F: detail of a regular-sized introvert scalid; G: Ventral neck view (arrows indicate the
553 placid width at base); H: Dorsal view of segments 10–11; I: Ventral view of segments 8–10.
554 Abbreviations: bs, basal sheath of scalid; dis, distal part (of outer oral styles); ep, end-piece of
555 scalid; lds, laterodorsal spine; ltas, lateral terminal accessory spine; lts, lateral terminal spine;
556 lvs, lateroventral spine; mds, middorsal spine; mts, midterminal spine; mvpl, midventral placid;
557 pro, proximal part (of outer oral styles); numbers after abbreviation indicate corresponding
558 segment.

559 Figure 4. Light micrographs of female adult holotype NHMD-1174547 (A, C–D, F–I) and
560 female adult paratype NHMD-672705 (B, E) of *Ryuguderes casarrubiosi* sp. nov., showing
561 trunk cuticular details of segments 1–7. A, B: Middorsal to laterodorsal view of segments 1–3
562 tergal plates; C: detail of the unpaired, paradorsal sensory spot of segment 4; D: detail of the
563 paired paradorsal sensory spots of segment 6; E: ventral view of segments 1–3; F: middorsal to
564 midlateral view of segments 4–5 tergal plates; G: lateroventral view of segments 5–6; H:
565 midlateral to midventral view of segments 6–7 cuticular plates; I: right sternal plate of segment
566 6. Abbreviations: las, lateral accessory spine; lvb, lateroventral blunt spine; lvs, lateroventral
567 spine; mds, middorsal spine; ppf, primary pectinate fringe; sp, sternal plate; spf, secondary
568 pectinate fringe; tp, tergal plate; vmpa, ventromedial papilla; numbers after abbreviation
569 indicate corresponding segment; glandular cell outlets are marked as continuous circles, and
570 sensory spots as dashed circles.

571 Figure 5. Light micrographs of female adult holotype NHMD-1174547 (A–E), female adult
572 paratype NHMD-672705 (I) and male adult paratype NHMD-672702 (F–H) of *Ryuguderes*
573 *casarrubiosi* sp. nov., showing trunk cuticular details of segments 6–11. A: Middorsal to
574 midlateral view of segment 8; B: right sternal plate of segment 8; C: midlateral to lateroventral
575 view of segments 9–10; D: middorsal to laterodorsal view of segments 10–11; E: right sternal
576 plates of segments 10–11; F: right sternal plates of segments 6–7; G: middorsal to laterodorsal
577 view of segments 10–11; H: right sternal plates of segments 10–11; I: ventral view of segment
578 11. Abbreviations: go, gonopore; lane, lateral accessory nephridiopore; lds, laterodorsal spine;
579 ltas, lateral terminal accessory spine; lts, lateral terminal spine; lvs, lateroventral spine; mds,
580 middorsal spine; mts, midterminal spine; po, pore; spf, secondary pectinate fringe; vmpa,
581 ventromedial papilla; numbers after abbreviation indicate corresponding segment; glandular
582 cell outlets are marked as continuous circles, and sensory spots as dashed circles.

583

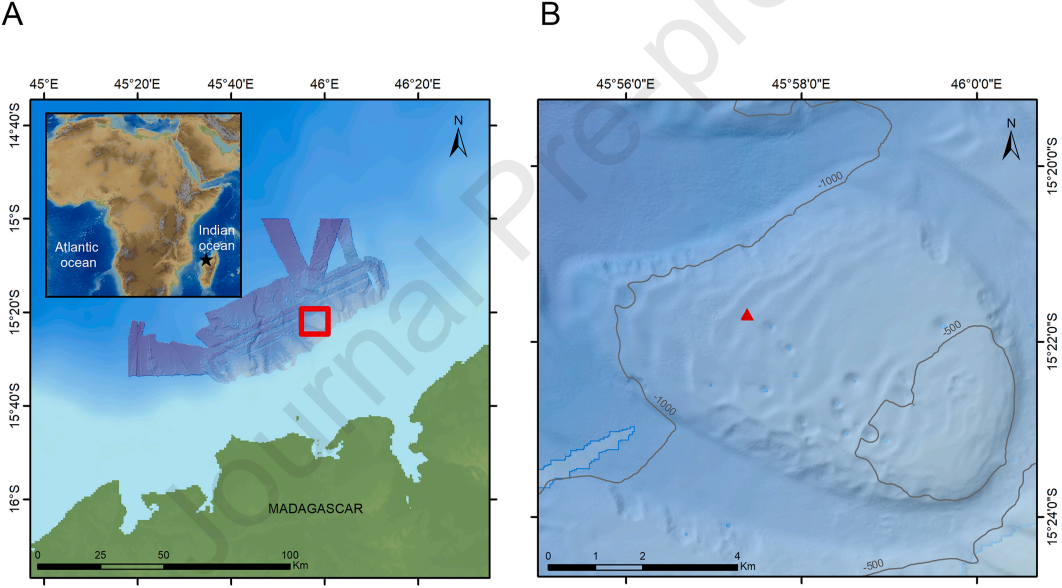
A
45°E
45°20'E
45°40'E
46°E
46°20'E
14°40'S
15°S
15°20'S
15°40'S
16°S
N
Atlantic ocean
Indian ocean
MADAGASCAR
0
25
50
100
Km
B
45°56'0"E
45°58'0"E
46°0'0"E
15°20'0"S
15°22'0"S
15°24'0"S
N
-1000
-500
-1000
-500
0
1
2
4
Km

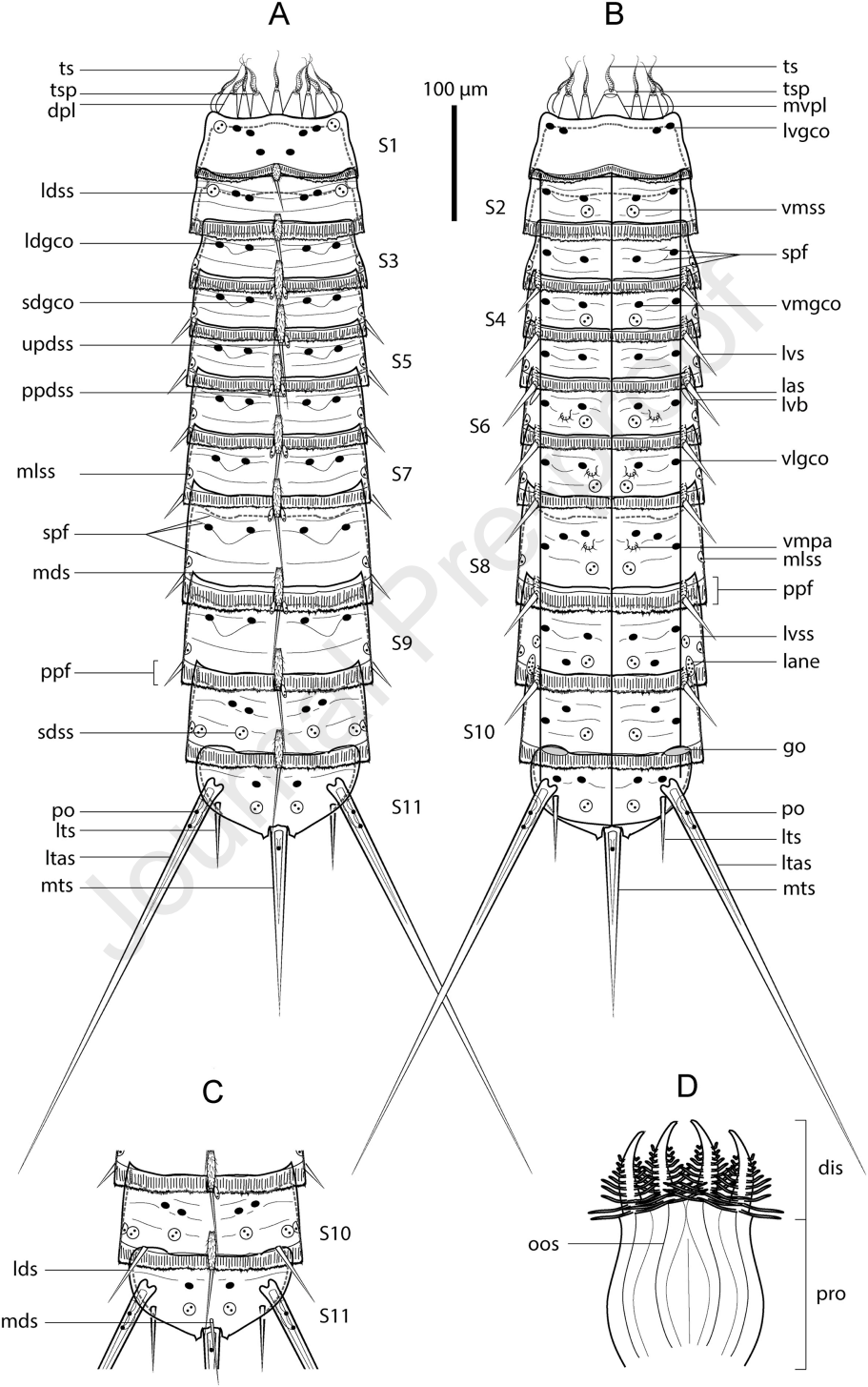
A
B
C
D
100 µm
ts
tsp
dpl
ldss
ldgco
sdgco
updss
ppdss
mlss
spf
mds
ppf
sdss
po
lts
ltas
mts
S1
S3
S5
S7
S9
S11
mvpl
lvgco
S2
vmss
spf
S4
vmgco
lvs
las
lvb
S6
vlgco
vmpa
mlss
S8
ppf
lvss
lane
S10
go
lds
S10
S11
oos
dis
pro

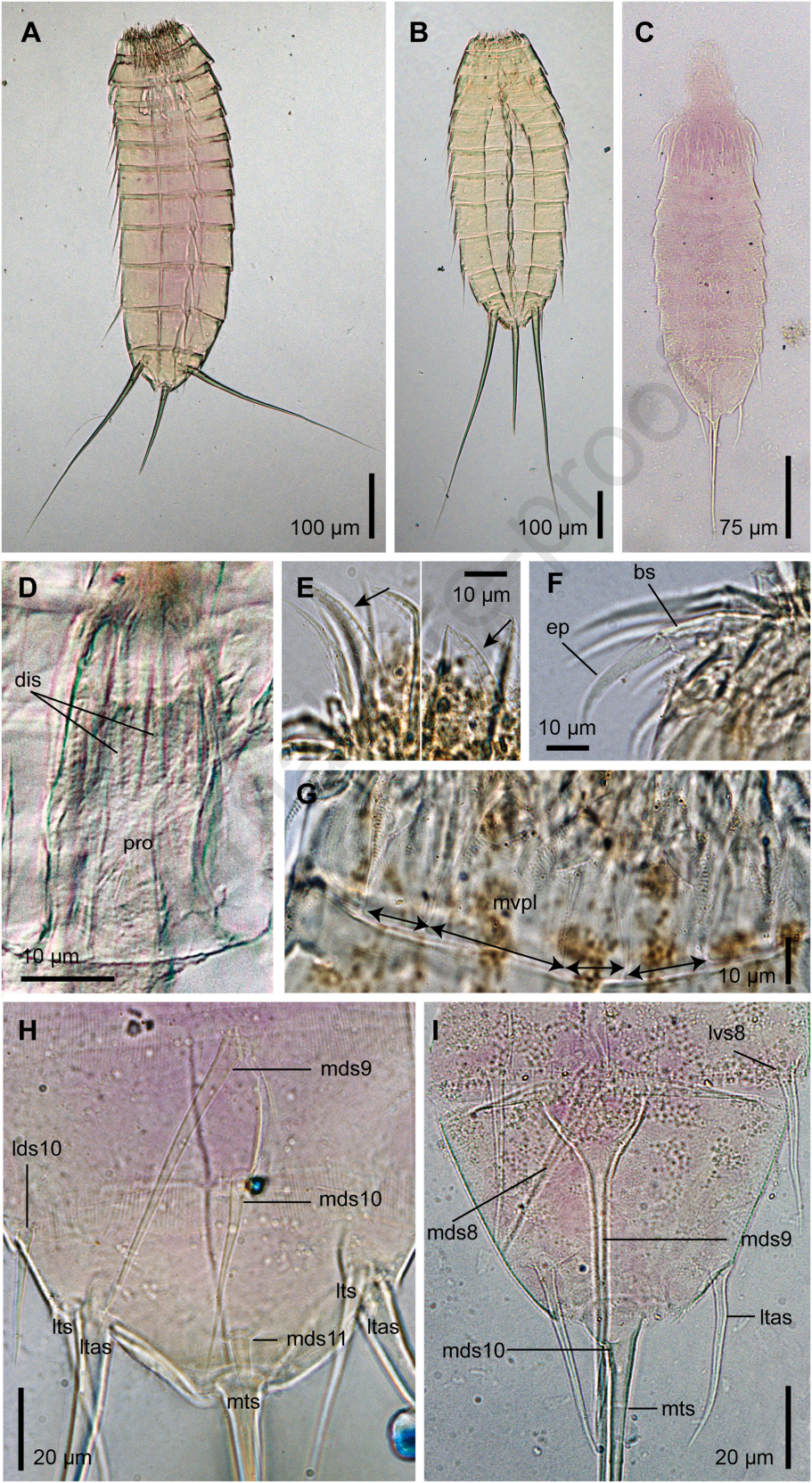
A
100 µm
B
100 µm
C
75 µm
D
dis
pro
10 µm
E
10 µm
F
bs
ep
10 µm
G
mvpl
10 µm
H
mds9
lds10
mds10
lts
lts
ltas
mds11
ltas
mts
20 µm
I
lvs8
mds8
mds9
ltas
mds10
mts
20 µm

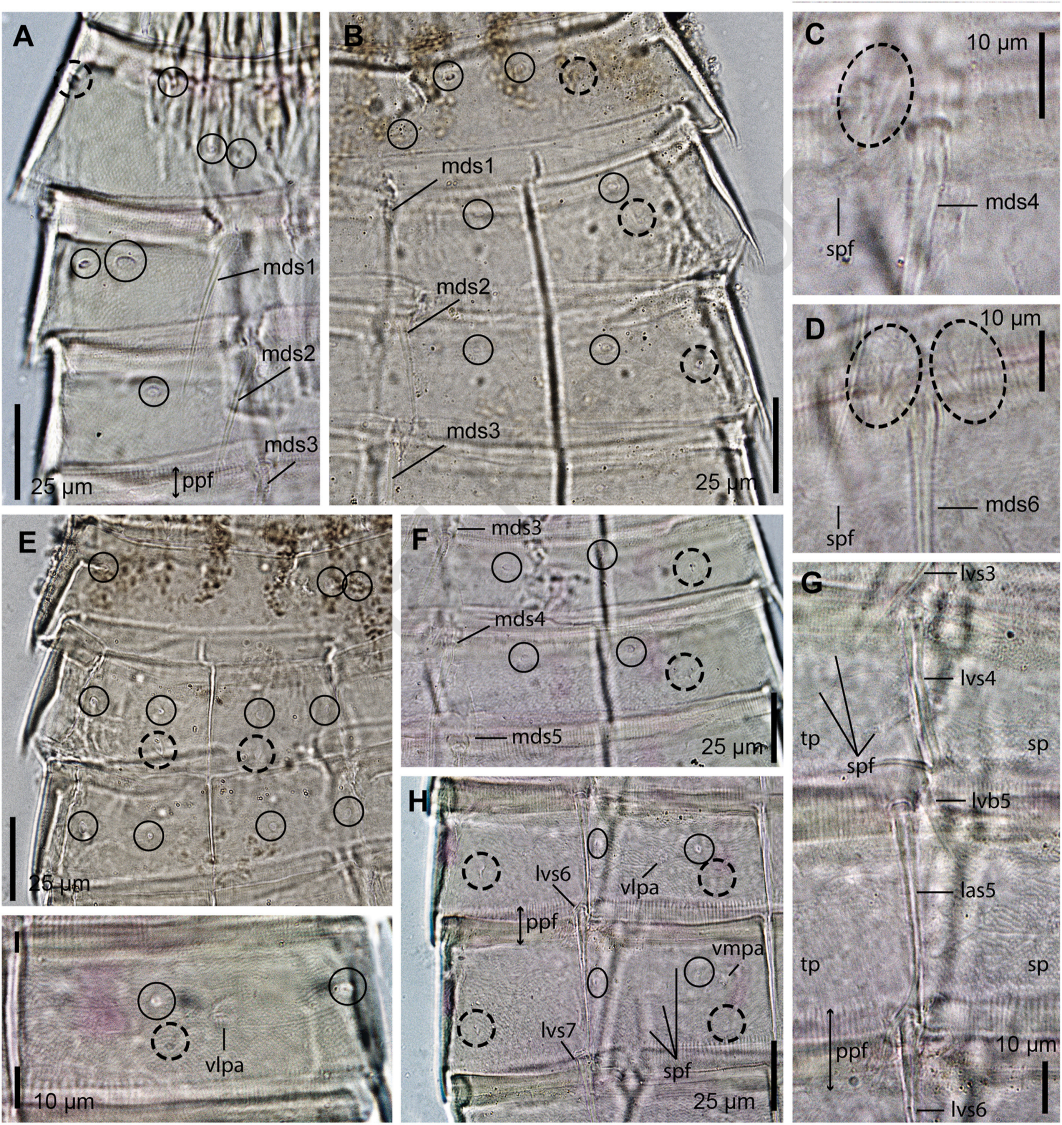
A
mds1
mds2
mds3
25 µm
ppf
B
mds1
mds2
mds3
25 µm
C
10 µm
mds4
spf
D
10 µm
mds6
spf
E
25 µm
F
mds3
mds4
mds5
25 µm
G
lvs3
lvs4
tp
spf
sp
lvb5
las5
tp
sp
ppf
10 µm
lvs6
I
vlpa
10 µm
H
lvs6
vlpa
ppf
vmpa
lvs7
spf
25 µm

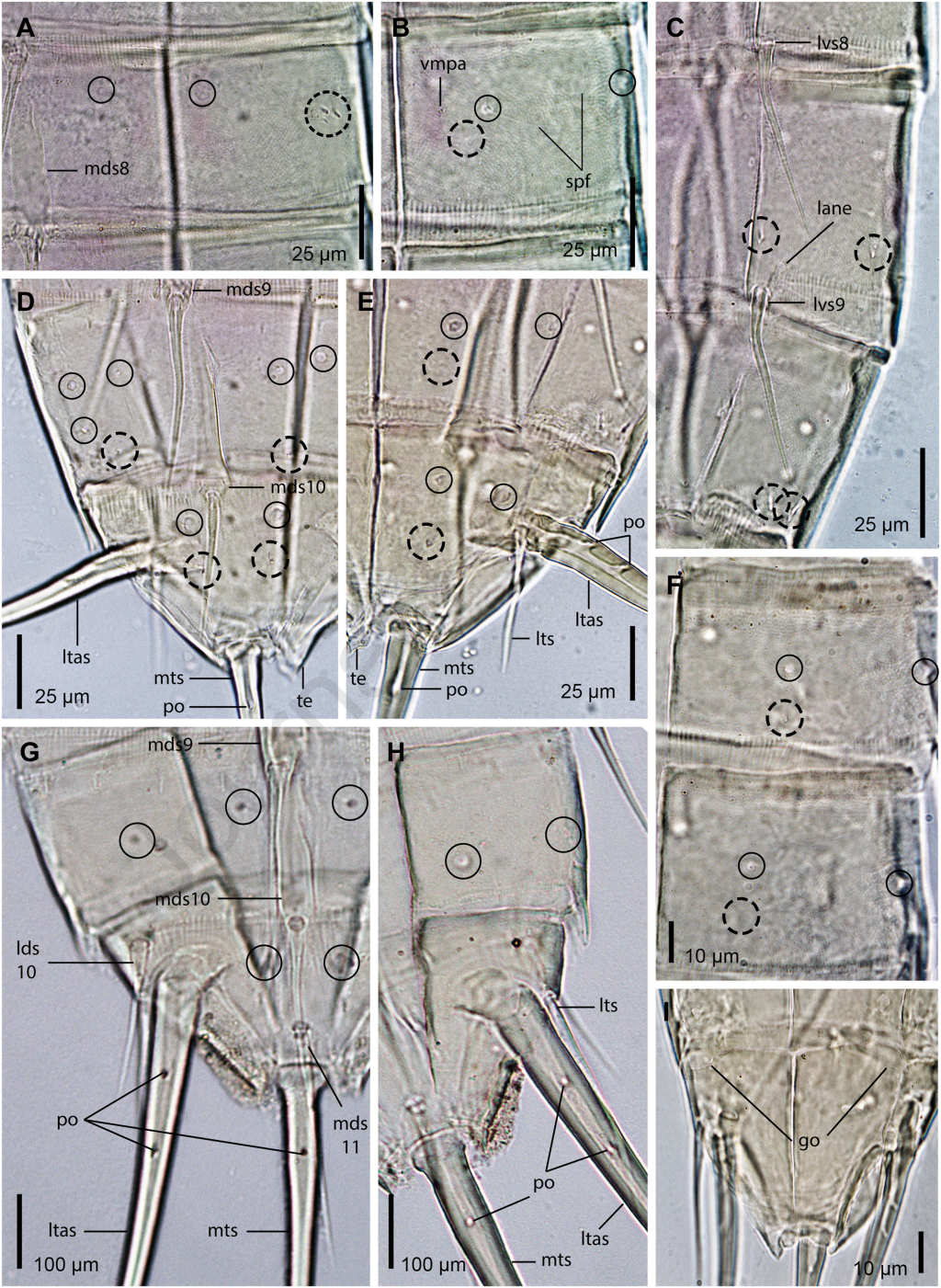
A
mds8
25 µm
B
vmpa
spf
25 µm
C
lvs8
lane
lvs9
25 µm
D
mds9
mds10
ltas
25 µm
mts
po
te
E
po
ltas
lts
te
mts
po
25 µm
F
10 µm
G
mds9
mds10
lds
10
po
mds
11
ltas
100 µm
mts
H
lts
po
ltas
100 µm
mts
I
go
10 µm

Declaration of interests

☒The authors declare that they have no known competing financial interests or personal relationships that could have appeared to influence the work reported in this paper.

☐The authors declare the following financial interests/personal relationships which may be considered as potential competing interests: